A PORTABLE VORTEX MIXER WITH OBJECT DETECTION SENSORS USING TFT ILI9341 CONTROL DISPLAY

Rinda Nur Hidayati[1*], Indra Gunawan[1], Atika Hendryani[1], Gita Rindang Lestari[1], Natasya H Salsabila[1]

[1]Department of Electromedical, Poltekkes Kemenkes Jakarta II, Jakarta, Indonesia, 12120

*E-mail: rinda_nurhidayati@poltekkesjkt2.ac.id

Submitted: 28th June 2023; Accepted: 23th August 2024

http://doi.org/10.36525/sanitas.2024.438

ABSTRACT

A vortex mixer can be utilized for repetitive sample-mixing tasks that need execution over a predetermined period. The subject of this study is a device known as a vortex mixer, which is used to rapidly homogenize liquids in a compact container. The module's design aims to produce a portable vortex mixer with an object detector for use in the solution-mixing process. The module comprises a circuit controlled by ESP32, an infrared sensor for object detection, and a TFT LCD ILI9341 for display. A charging battery can also charge this device, making it easier to transport. This instrument has three degrees of speed: the low-level ranges from 300 to 500 RPM, the medium level ranges from 600 to 1500 RPM, and the high level extends from 1600 to 2500 RPM. The results reveal that the motor speed accuracy of the vortex mixers is low at 95.78%, medium at 97.49%, and high at 99.19%. Moreover, the battery life is lengthy, with an average charging time of 2.62 hours and a discharging time of 9.7 hours for 300 RPM; 7.34 hours for 600 RPM; and 3.03 hours for 1600 RPM, respectively.

Keywords: *Vortex mixer, ESP32, Infrared sensor, Mixing solution, RPM*

INTRODUCTION

The technology industry is currently very focused on developing technology to suit society's increasing needs and demands. All aspects of supporting human activities must be sophisticated, practical, and automatic, and of course, electricity saving is also included to make work easier (1). According to the Regulation of the Minister of Health of the Republic of Indonesia No. 43 of 2013 clause 1 verse (1), a clinical laboratory is a health laboratory that carries out clinical specimen examination services to obtain information about individual health, primarily to support the diagnosis of disease, cure of disease, and recovery of health (2). One of them is the process of mixing samples in the inspection service.

Self-mixing is a process of homogenizing two or more types of liquids in a container. It is called mixing because its arrangement or composition is subject to change. It is called homogeneous because its structure is so uniform that it cannot be observed in the presence of different parts, even with an optical microscope (3)(4). This mixing can be done manually, commonly called the finger vortex. Finger vortex is done by closing the tube using a finger which is then moved up and down repeatedly. Usually, this finger vortex method takes longer and often results in inadequate suspense. The inefficient process is primarily related to small quantities of reagents. So that if the mixing process is done manually, it will be less efficient in both time and energy, coupled with the presence of harmful liquids that should not be in direct contact with the skin. Therefore, to make up for the shortcomings caused by the finger vortex, a more practical tool was developed, namely the vortex mixer (5)(6).

A vortex mixer is a health support device in the form of a mixer that rotates like a whirlpool or wind to quickly homogenize or mix liquids in a small container (7). Small containers used such as test tubes, centrifuge tubes, Eppendorf, falcon, or other small containers. This tool can mix small samples up to 50 ml in size with a speed range of up to 3000 RPM (8). This device is commonly used in bioscience laboratories and is frequently used in the destruction of the substance at the time of preparation of reagent manufacturing. This device is equipped with speed control that can be adjusted as needed (9).

Mixers with low speed are usually used for liquids with high viscosity where the mixture is concentrated, slippery, and so on, like thick oil and sludge where some fibres or liquids can cause foam. High speed is usually used for liquids with low viscosity, e.g., water. Medium speed is generally used for solutions such as thick syrup and lacquer oil. The safety of the process and the mixer speed are determined by the viscosity of the fluid and the geometric size of the mixer system contained in the table below (9)(10).

Table 1 Speed for Mixing Solution

RPM	Types of solution mixtures
≤500	For solutions that have a viscosity of less than <50cP
≤1000	For solutions that have a viscosity of more than >200cP
≤2000	For solutions that have low viscosity like water

Over these past five years, Vortex Mixer has been developed by Leni Astuti (2019) entitled, "Vortex Mixer Otomatis Berbasis Mikrokontroler Atmega328". In this study, the accuracy of the speed readings still needed to be improved, and the error obtained was quite large (7). In the previous research by Angger Trisna Andimi (2020), "Vortex Mixer Dilengkapi Tampilan RPM dan Pendeteksi Tabung". In this study, it is necessary to develop research to be more attractive and design portable or using batteries. Vortex mixer devices on the market or in the laboratory generally still use push buttons, rotary potentiometers or dimmers as speed settings. Then, the tube container immediately rotates even though there is no tube. It can be unsafe when the tube is laid because it has the potential to reflect the tube (9). In addition, the author has yet to find a vortex mixer that can be operated portable or with rechargeable batteries as its power source. Rechargeable batteries as an alternative power source are prevalent in various technologies. Its long-lasting and environmentally friendly use that saves more electricity and does not require large amounts of electricity for recharging makes it more in demand (11).

Based on this background, the author is interested in further developing a vortex mixer device with speed settings according to the user's wishes which are displayed and run through a touchscreen display with an infrared sensor as an automatic drive of the motor when an object is detected to facilitate the user in use and reduce the possibility of lousy tube bounces. The author uses an infrared sensor because it has a minimal distance detection range to detect the distance that the author wants and does not detect other objects that are not needed (12). This device uses battery power as the primary voltage source to make it easier for the tool to be used when there is a power failure and does not take up space in the outlet, saving electricity use.

RESEARCH METHOD

A. Experimental Setup

This study estimates speed values at three different speeds: with five repetitions of data retrieval, the motor speed is indicated by the low level, which ranges from 300 to 500 RPM; the medium level, which ranges from 600 to 1500 RPM; and the high level, which ranges from 1600 to 2500 RPM. The speed is then set using the display. This investigation utilized an ESP32 to control the module's overall operation, an FC-51 sensor to detect an object or sample when it was placed in the tube container, a TFT ILI9341 to display and set the speed, a button on the TFT to select and start the device, a battery to provide voltage to the module, a motor DC to rotate the sample, and a driver motor BTS 7960 to operate the motor DC. After the design was complete, a tachometer was used to compare the speed values in the module and the display. The test is taken by placing the sample in the tube container for object detection. The motor will rotate and mix the sample when the sensor detects an object. A stopwatch is then used to measure the charging and discharging times of the battery to determine its lifetime.

B. The Diagram Block

Figure 1 is a block diagram of the module's operation. In this study, a 12V battery is connected to the DC power supply. When the battery's condition deteriorates, the charger circuit receives power from the PLN and charges the battery. There is an on/off switch; the device will be operational when the switch is in the on position. The battery provides voltage to the entire circuit when the switch is in the on position. The microcontroller will control the operation of the entire circuit, and after initialization and activation, the LCDs have the selected speed. You can adjust the speed via the TFT LCD, and the microcontroller will receive the result. After processing the tube, the object detection sensor will instruct the microcontroller to apply voltage to the motor driver. It will cause the motor to move, resulting in the rotation of the sample tube and a mixing process. During the mixing process, the motor driver stops the rotating motor when it no longer detects the tube.

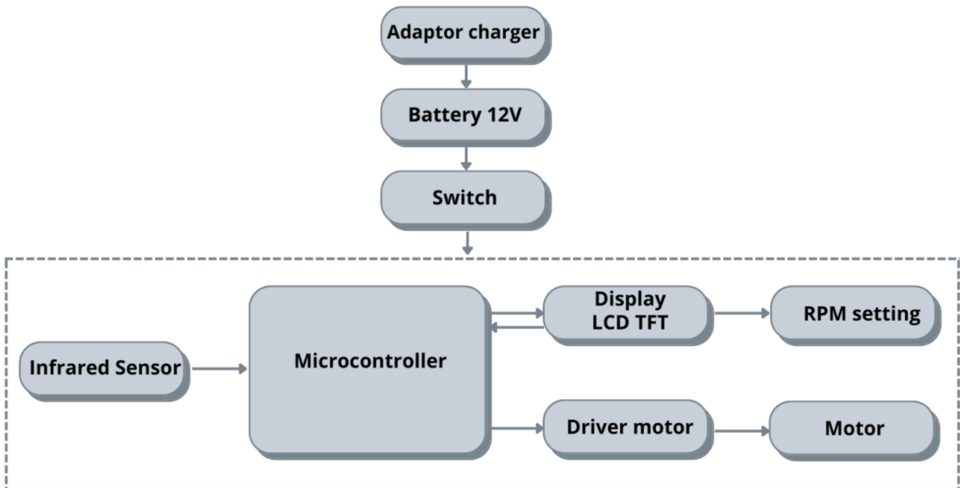

Figure 1 Diagram block of the module operation

C. Principle of Vortex Mixer Module

Figure 2 is a flowchart that served as the foundation for the development of the program. The switch is pressed into the on position, the tool will turn on, and the LCD will start initializing and an initial display recognition. By pressing "NEXT," the LCD will switch to the next screen, which will display the RPM setting. After adjusting the desired RPM setting, press the start button. When the sensor detects the presence of a tube, the motor will begin working, and the mixing process will begin. If neither the object nor the tube is detected, the microcontroller will instruct the motor to stop.

D. The Circuit Diagram

This circuit diagram in Figure 3 represents a considerable portion of this study. The hardware design for this vortex mixer consists of an ESP32 microcontroller, an LCD TFT ILI9341 display and setting device, an object detection infrared sensor module, a BTS7960 motor driver, a driver DC motor for rotating the sample, a step-down DC to DC motor, and a battery. Using a programmed microcontroller, a TFT ILI9341 LCD, the process of setting the desired speed in the module design. The LCDs the module's operation, from when it is turned on to when it is turned off.

This circuit controls the speed of the DC motor by employing the PWM method. The module uses a DC motor and the BTS7960 motor driver. This circuit utilizes the FC-51 infrared object detection sensor. This circuit is used for tube detection. When a tube is placed in the container, the sensor will detect it and convert the electrical signals into binary data, decoded and used to convert the analog data to digital data (ADC). Because the ADC results are sent to the ESP32 microcontroller, the motor can rotate. The entire circuit was designed using Easyeda as shown in Figure 3.

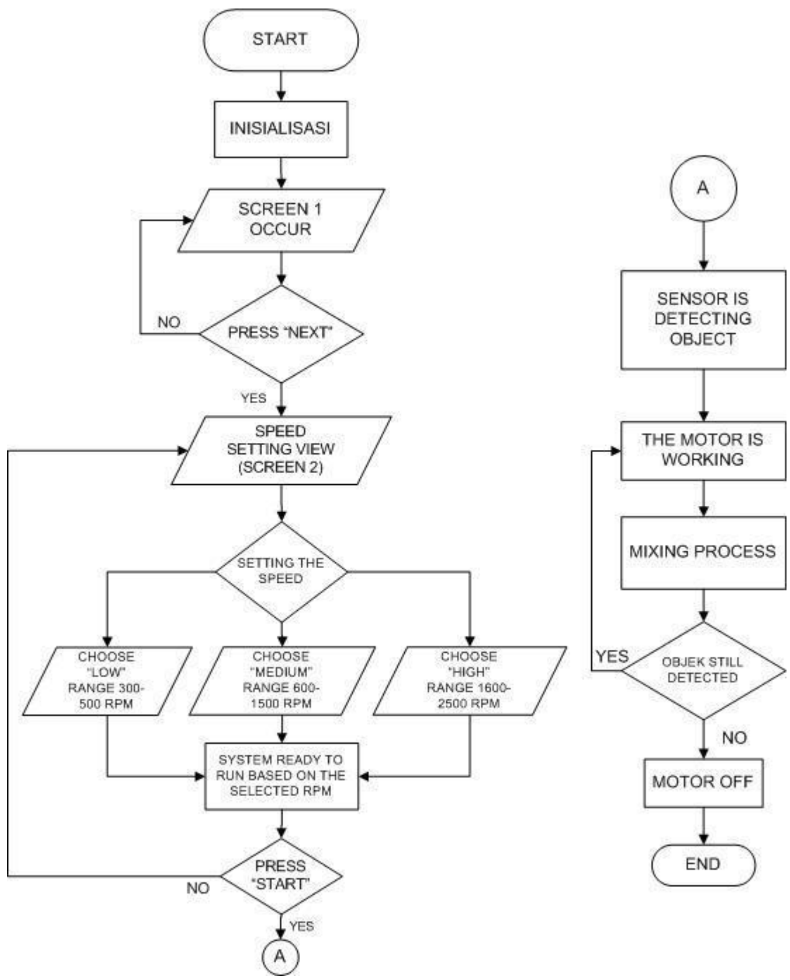

Figure 2 Flowchart of the working principle of the module

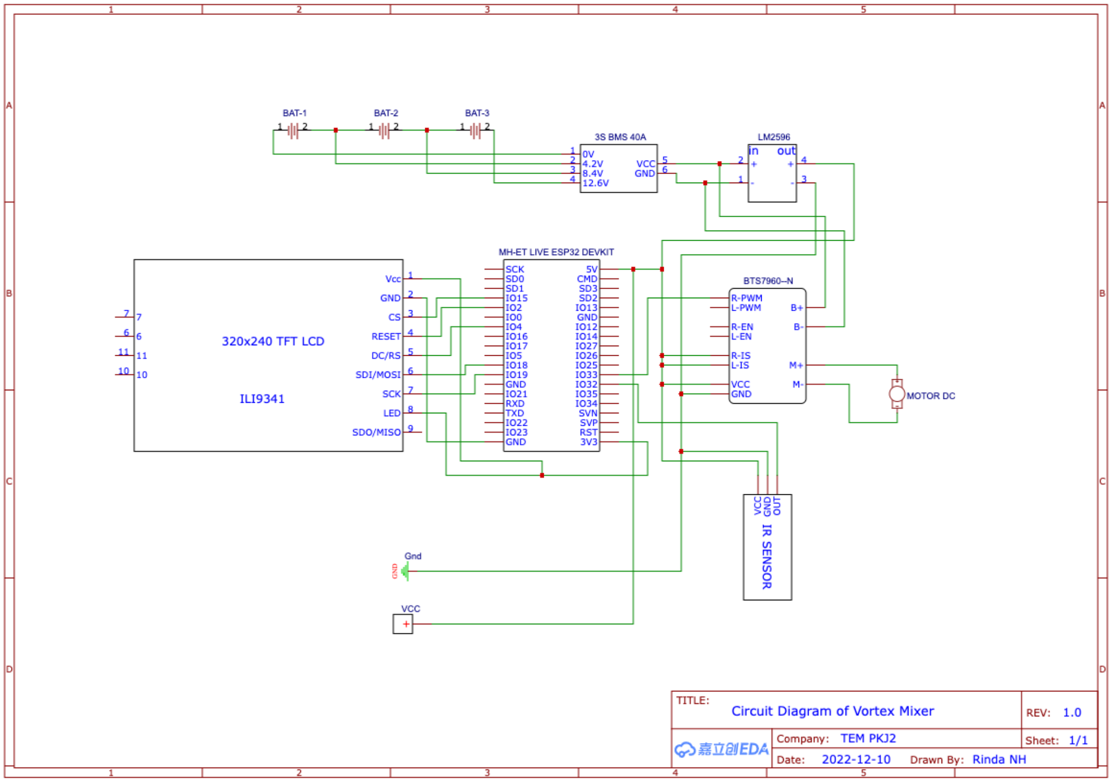

Figure 3 The circuit diagram of vortex mixer design

1. BMS (Battery Management System)

This research examines several aspects of the battery, including its voltage, capacity, the time it takes to function after being fully charged, and maximum load capacity. It is necessary to collect information sources based on the specifications of the active components; for DC motors, this information is provided when the maximum speed is reached, and planning for batteries begins with the following calculation of battery load power:

Table 2 Reference Data of Power and Electrical Current

Component	Power (V*I)
Motor DC + Driver	12 VDC x 3A = 36 W
ESP32	3.3 VDC x 0,05A = 0,165 W
Step down DC to DC	5 VDC x 3A = 15 W
FC-51	5 VDC x 0,043 A = 0,215 W
TFT ILI9341	3.3 VDC x 0,48 A = 1,584 W
Power	52,964 W
Electrical Current	6,573 A

According to Table 2, the vortex mixer requires 6.5 A of current and 52.964 W of power. The calculation is based on the theoretical maximum amount, which has been modified to meet the current needs. The subsequent step is to choose a Li-ion battery (13) whose capacity corresponds to the maximum current and the cost. This study selects three Li-Ion batteries with a capacity of 3Ah and a voltage of 3.7 volts (14,15). If the battery is arranged in series, the voltage will increase, while if it is arranged in parallel, the capacity will increase. The series connection of the three batteries produces a total of 12V and 3Ah.

2. Power Supply

The supply is a DC voltage source that provides voltage to the entire circuit. In this study, 12VDC and 5VDC were required to power the entire circuit. Using step-down DC to DC, a lithium-ion battery is connected in series to produce a voltage that can power a 12V DC motor and other circuits. Figure 3 depicts the pins utilized for this series.

A BMS (Battery Management System) is required to ensure the tool's safety by preventing overcharging and over-discharging of the 12V battery before the voltage reaches the entire circuit. The BMS consists of circuits for overcurrent, overvoltage, short circuit protection, cell balancing, and disconnecting the BMS from the battery. If one of the batteries has a voltage below 3.0V, the BMS mosfet will open to maintain over-discharge and protect against a cycle life voltage of 10V. Through the BMS's resistor and transistor, there is also a voltage balancer between cells so that they will be charged equally when it is charged. The voltages at P+ and P- are 12 volts. The P+ and P- outputs will be displayed on an LCD TFT, in addition to serving as battery indicators and charger inputs.

E. The Design of Vortex Mixer

The shell for the vortex mixer is designed using the Fusion 360 application. The design outcomes are depicted as 3D representations in Figures 4.

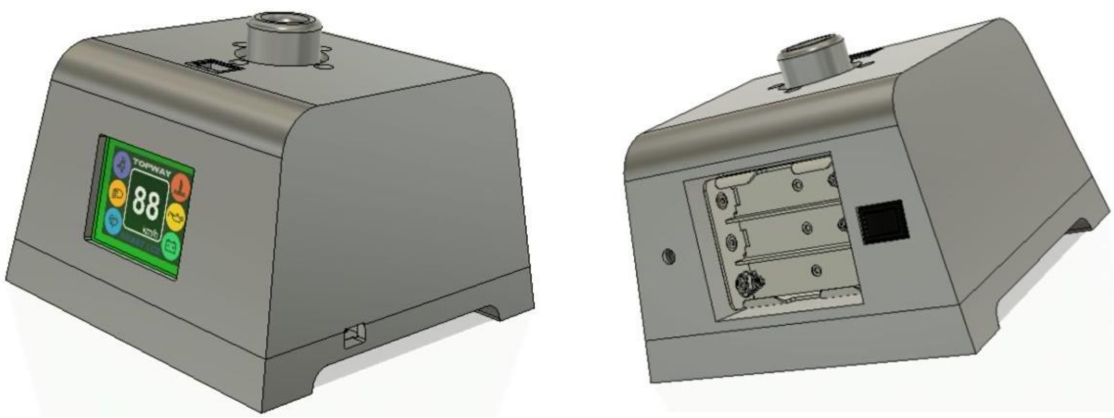

(a) (b)

Figure 4 Casing design (a) front view (b) back view

Spesifications:

Material	: PLA and ABS - Printer 3D and Rubber
Dimension	: 17x17x9 cm

Technical spesifications:

Module's name	: Vortex Mixer Portable
Power supply	: ± 220 V AC, 50/60 Hz
	±12 V DC
Display	: TFT LCD ILI9341
Speed	: 300-500 RPM (low), 600-1500 (medium), 1600-2500 RPM (high)
Mixing motion	: Orbital/Vortex
Tube sensor	: Infrared
Microcontroller	: ESP32
Motor type	: Motor DC Brushed 12V
Rechargeable battery	: Lithium-Ion
Material	: 3D Printing dan rubber (tube container)
Tool's dimension	: 17x17x9 cm
Tube container dimension	: diameter 5 cm
Tube volume	: ~50 ml

RESULTS AND DISCUSSION

This section will examine whether the data obtained using the designed module will be presented as expected. The obtained data are then processed in order to produce an accurate data analysis. In the introduction to this data, it tends to be determined whether the rotational speed of the engine will remain constant during operation, whether the FC-51 module is effective in tube identification, whether the touchscreen is functioning correctly, and whether the battery life by testing one of the rates at each speed level.

A. The Result of motor speed measurement

The motor's parameters are measured at three different speeds: low (300-500 RPM), medium (600-1500 RPM), and high (1600-2500 RPM), and the results are displayed on the TFT LCD of the module.

Table 3 shows motor speed measurements for each speed level up to five times using a tachometer, with a variance of 100 RPM between readings. The results of comparing the RPM speed settings with the speed measurement results can be seen in Figure 5, that the linearity obtained by R^2 0.99 is close to the linearity value of 1.

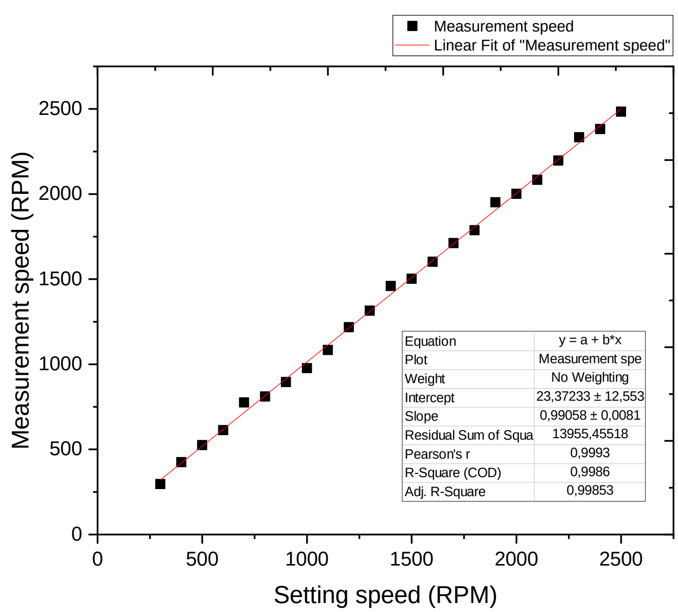

Figure 5 Linearity of speed settings and speed measurement results

Table 3 The Result of Measuring Speed

Speed Level	Setting Speed (*RPM*)	The i-mesurement (*RPM*) 1	2	3	4	5	$\bar{X}$	Error	% Error	Accuration
LOW	300	283	288	301	304	305	296.2	3.8	1.27%	98.73%
	400	440	440	354	443	448	425	25	6.25%	93.75%
	500	566	438	479	573	572	525.6	25.6	5.12%	94.88%
	Average								**4.21%**	**95.78%**
MEDIUM	600	607	620	608	612	617	612.8	12.8	2.13%	97.87%
	700	830	717	867	732	732	775.6	75.6	10.80%	89.20%
	800	820	798	798	840	798	810.8	10.8	1.35%	98.65%
	900	863	904	904	904	904	895.8	4.2	0.47%	99.53%
	1000	975	1024	937	923	1028	977.4	22.6	2.26%	97.74%
	1100	1073	1007	1134	1068	1136	1083.6	16.4	1.49%	98.51%
	1200	1214	1230	1217	1187	1243	1218.2	18.2	1.52%	98.48%
	1300	1233	1360	1383	1255	1344	1315	15	1.15%	98.85%
	1400	1492	1333	1492	1492	1492	1460.2	60.2	4.30%	95.70%
	1500	1494	1494	1508	1514	1503	1502.6	2.6	0.17%	99.83%
	Average								**2.56%**	**97.44%**
HIGH	1600	1665	1587	1587	1587	1587	1602.6	2.6	0.16%	99.84%
	1700	1731	1676	1717	1717	1717	1711.6	11.6	0.68%	99.32%
	1800	1794	1763	1792	1794	1793	1787.2	12.8	0.71%	99.29%
	1900	1876	1973	1971	1971	1968	1951.8	51.8	2.73%	97.27%
	2000	1869	2031	2090	1970	2047	2001.4	1.4	0.07%	99.93%
	2100	1950	2241	2094	2022	2114	2084.2	15.8	0.75%	99.25%
	2200	2272	2283	2283	2029	2117	2196.8	3.2	0.15%	99.85%
	2300	2442	2350	2299	2312	2266	2333.8	33.8	1.47%	98.53%
	2400	2399	2341	2327	2392	2451	2382	33.8	0.75%	99.25%
	2500	2467	2467	2544	2531	2412	2484.2	18	0.63%	99.37%
	Average								**0.8%**	**99.19%**

B. The result of effectiveness testing of the infrared sensor

The infrared sensor efficiency in object detection is tested by placing the object on top of the sensor; if the sensor detects the thing, the motor turns, and the sensor turns on. According to table 4, measuring the FC-51 infrared sensor's ability to detect the tube five times determined that the tube is seen and automatically starts and stops the motor.

Table 4 The Result of the Infrared Sensor Efficiency

i-measurement	Tubeless condition	There is a tube
1	Sensor off	Sensor on
2	Sensor off	Sensor on
3	Sensor off	Sensor on
4	Sensor off	Sensor on
5	Sensor off	Sensor on

C. The result of the button function on the LCD TFT

The buttons' functionality can be examined by pressing the buttons on the TFT LCD panel. If pressing the button on the screen causes the settings to function and the tool to operate as expected, then the button is functioning correctly. Based on table 5.'s testing of the buttons on the TFT LCD, it is evident that the buttons can be used to adjust the instrument.

Table 5 The Result of Testing the Button Function

Screen	Button	Result		
		1	2	3
1	*NEXT*	✓	✓	✓
2	*LOW*	✓	✓	✓
	MEDIUM	✓	✓	✓
	HIGH	✓	✓	✓
	UP	✓	✓	✓
	DOWN	✓	✓	✓
	START	✓	✓	✓
	BACK	✓	✓	✓

Explanation:
✓ = Successfully pressed
X = Failed to be pressed

D. The result of the battery lifetime

The button's functionality can be examined by pressing the buttons on the TFT LCD panel. If pressing the button on the screen causes the settings to function and the tool to operate as desired, we may say that the button is functional. The charge time is measured five times at a consistent pace while the device is turned off, and the discharge period is measured five times at a constant speed. For discharging time testing, 300 RPM for low speed, 500 RPM for medium speed, and 1600 RPM for high speed are measured until the remaining battery percentage reaches 20%.

Following table 6, the average charging time is 157.6 minutes or 2.62 hours, based on five tests of the battery's lifespan. Based on table 7, the average time for 300 RPM, 600 RPM, and 1600 RPM is 581.6 minutes or 9.7 hours, 440.2 minutes or 7.34 hours, and 181.6 minutes or 3.0 hours, respectively.

Table 6 The Result of Charging Time of the Battery

i-measurement	Charging time (minute)
1	159
2	149
3	162
4	151
5	167
Average	**157,6**

Table 7 The Result of Discharging Time of the Battery

Speed (RPM)	Discharging time (minute)					Average
	1	2	3	4	5	
300	585	591	578	571	583	**581,6**
600	457	431	435	449	429	**440,2**
1600	177	186	163	205	179	**182**

CONCLUSION

It was designed to implement a portable vortex mixer with an object detection sensor. The Laser Photo Tachometer was used to test the rotational speed accuracy. The results were satisfactory: the low level of 95.78%, the medium level of 97.49%, and the high level of 99.19%. The battery has an average charge life of 2.62 hours, and its discharge time varies depending on speed: 9.7 hours at 300 RPM, 7.34 hours at 600 RPM, and 3.03 hours at 1,600 RPM. In addition, the fact that the motor rotates when the tube is detected demonstrates that the infrared sensor can detect it effectively.

REFERENCES

1. Riandi R, Brillian Kharisma O, Ullah A. Pengembangan Sistem Deteksi Objek berbasis Teknologi Internet of Things terintegrasi Telegram Bot menggunakan Ultrasonik HCS04R. Semin Nas Teknol Informasi, Komun dan Ind. 2018;(11):2579–5406.
2. Permenkes. PMK-RI No.65 Th.2016 Standart Pelayanan Elektromedik. Stand Pelayanan Elektromedik. 2016;(2016):46.
3. Rogovyi A, Korohodskyi V, Khovanskyi S, Hrechka I, Medvediev Y. Optimal design of vortex chamber pump. In: Journal of Physics: Conference Series. IOP Publishing Ltd; 2021.
4. Fischer M, Chakravarty S, Le Bihan O, Morgeneyer M. Parametric study of the particle motion induced by a vortex shaker. Powder Technol. 2020:1(374):70–81.
5. Patel AK, Henry R, Jha A, Patwardhan A, Pawar J. Design and Fabrication of Low Cost Vortex Mixer Using Additive Manufacturing Synthesis of metal oxide nanoparticles for Biological applications. View project Design and Fabrication of Low Cost Vortex Mixer Using Additive Manufacturing. Int J Res Advent Technol. 2018;6(12):3513-3516.
6. Mejia-Ariza R. Design, Synthesis, and Characterization of Magnetite Clusters using a Multi Inlet Vortex Mixer. Blacksburg, Virginia; 2010.
7. Astuti L. Vortex Mixer Otomatis Berbasis Mikrokontroler ATmega328. J TEMIK (Teknik Elektromedik). 2019;3(3):22–39.
8. Yang AS, Hsieh YF, Kuo LS, Tseng LY, Liao SK, Chen PH. A novel vortex mixer actuated by one-shot electricity-free pumps. Chem Eng J. 2013:5(228):882–8.
9. A. N. Aisyah, E. D. Setionigsih, and Lamidi a. Vortex Mixer Live Rpm Dilengkapi Sensor Pendeteksi Tabung. J Tek Elektromedik. 2017;1(10).
10. Barabash VM, Abiev RS, Kulov NN. Theory and Practice of Mixing: A Review. Vol. 52, Theoretical Foundations of Chemical Engineering. Maik Nauka Publishing/Springer SBM; 2018. p. 473–87.
11. A.C. dan Q.R. Ramadani. Tujuh Alat yang Bisa Bantu Menghemat Biaya Listrik.

2021 Mei 26; Available from: https://www.republika.co.id/berita/qo09je425/tujuh-alat-yang-bisa-bantu-menghemat-biaya-listrik

12. Yunardi RT. Analisa Kinerja Sensor Inframerah dan Ultrasonik untuk Sistem Pengukuran Jarak pada Mobile Robot Inspection. Setrum Sist Kendali-Tenaga-elektronika-telekomunikasi-komputer. 2017;6(1):33.
13. Jaguemont J, Darwiche A, Bardé F. Optimal Fast-Charging Strategy for Cylindrical Li-Ion Cells at Different Temperatures. World Electr Veh J. 2024 Jul 24;15(8):330.
14. Jaguemont J, Darwiche A, Bardé F. 2024. Optimal fast-charging strategy for cylindrical Li-ion cells. 2024:15(8):1-14.
15. Liu Y, Liao YG, Lai MC. Effects of battery pack capacity on fuel economy of hybrid electric vehicles. In: 2021 IEEE Transportation Electrification Conference and Expo, ITEC 2021. Institute of Electrical and Electronics Engineers Inc.; 2021. p. 771–5.